Spatial Variation of the Regional Wind Field with Land–Sea Contrasts and Complex Topography

KYUNG-JA HA AND SUN-HEE SHIN

Division of Earth Environmental System, Pusan National University, Busan, Korea

LARRY MAHRT

College of Oceanic and Atmospheric Science, Oregon State University, Corvallis, Oregon

(Manuscript received 27 August 2008, in final form 18 March 2009)

ABSTRACT

This study examines the spatial variation of the wind field observed in the coastal zone of southeast Korea with its complex terrain, using measurements from a regional network 75 km across and centered about Busan. Results are compared with observations from an inland regional network centered around Daegu, Korea, with less dramatic, but still significant, surface heterogeneity. The coherency between stations is examined in terms of the between-station correlations of the wind components for all pairs of stations as a function of separation distance between stations. A mesovelocity scale is defined as a measure of the spatial variability of the wind field within the network. This variability is related to wind speed and cloud cover for the two contrasting regional networks. Additional comparisons are made with a homogenous rural network in Iowa. The results underscore the complexity of flow with topography, urban areas, and land–sea contrasts and demonstrate the inadequacy of existing network strategies.

1. Introduction

The variation of the wind field over heterogeneous surfaces has been examined primarily for well-defined surface discontinuities that sometimes lead to the formation of internal boundary layers, as occurs with abrupt changes in surface roughness or heat flux (e.g., Garratt 1990). Studies of simple surface heterogeneity have provided at least a partial understanding of the principal physics. Substantial progress has also been made in understanding thermally driven flows over well-defined slopes (Whiteman 2000). Less progress has been made with more complex terrain and disorganized surface heterogeneity (see references in Mahrt 2000). In this study, we will examine the spatial variations of the regional wind field within complex terrain and the suitability of existing networks for describing such spatial variability.

More complex surfaces include land–sea contrasts, topography, and urban areas (Pino et al. 2004). While considerable progress has been made toward understanding some elements of the vertical structure and turbulence quantities at a fixed location in the urban area (e.g., Roth 2000; Grimmond and Oke 2002; Kastner-Klein and Rotach 2004; Hanna et al. 2007), much less is known about the horizontal structure of the flow, except for relatively well-defined local circulations such as marine air penetration (e.g., Steyn 2002).

The first requirement for a network is that adjacent stations are to some degree correlated. If the spatial resolution is too crude to define a network, the stations are relatively independent of each other (Staebler and Fitzjarrald 2004). A given observational network may satisfy this coherence condition with stronger winds, but fail the coherency condition with weak large-scale flow and clear skies, when local microscale conditions dominate the wind field. Here, microscale conditions include the siting with respect to local features such as isolated vegetation elements and buildings. Because of these complications, the basic coherence between stations must be examined along with the suitability of data as a viable network. As a consequence of such difficulties, more sophisticated techniques for attempting to isolate certain types of horizontal coherent patterns (e.g.,

Corresponding author address: Kyung-Ja Ha, Division of Earth Environmental System, Pusan National University, Busan 609-735, Korea.
E-mail: kjha@pusan.ac.kr

DOI: 10.1175/2009JAMC2105.1

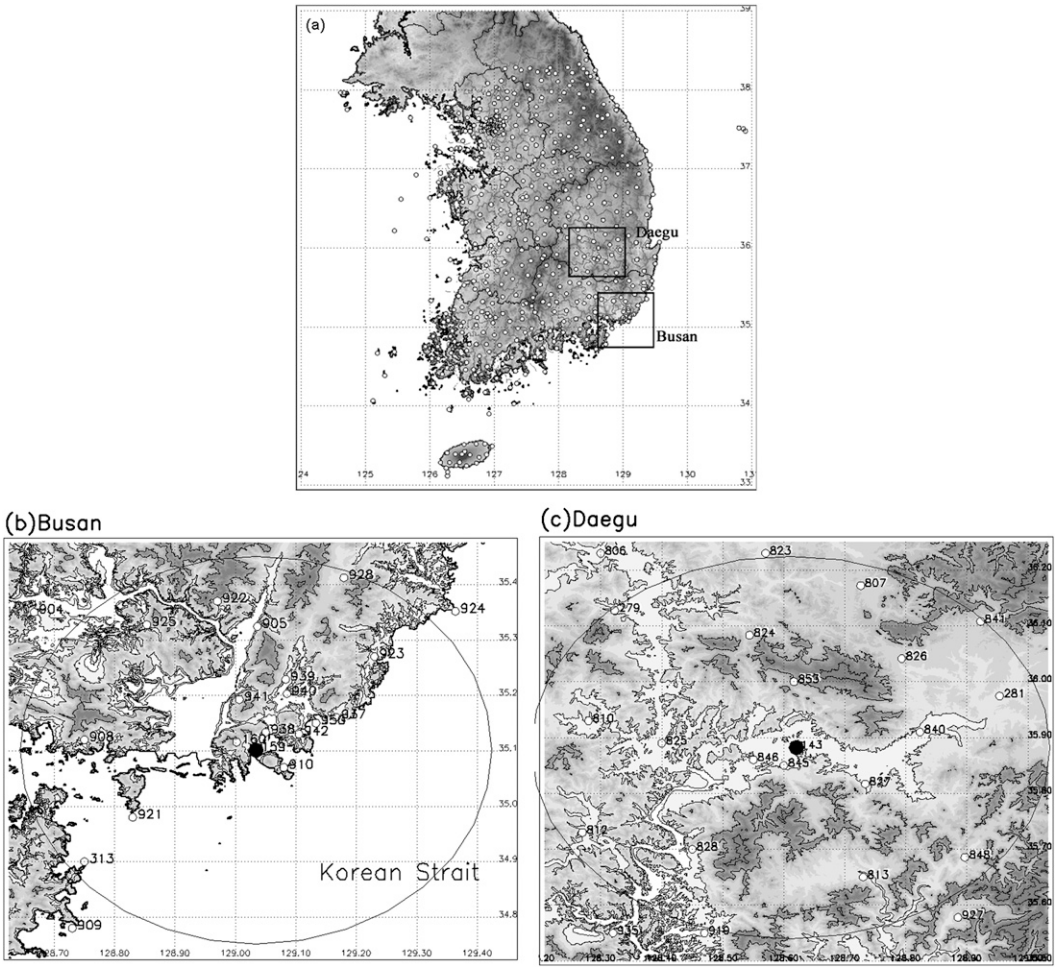

FIG. 1. The station distribution (open circles) on the (a) Korea peninsula, (b) Busan regional network, and (c) Daegu regional network. The large circle indicates the boundary of analyzed stations. The filled circles indicate regular synoptic stations in the Busan and Daegu networks. The elevation contours correspond to sea level, 10, 50, 400, and 800 m.

Ludwig et al. 2004; Beaver and Palazoglu 2006) will not be pursued here in favor of a more basic assessment of the overall coherence for different conditions. Our analysis will concentrate on two regional networks that include complex terrain, land–sea contrasts, and embedded urban areas, described in the next section.

2. The data

We analyze the 1-h data from the Busan and Daegu regional networks (Fig. 1) collected between 1 January 1999 and 1 November 2006 (Ha et al. 2007). Some of the calculations will be performed only for the ''goodset'' data, that is, only hourly records where data from all of the stations are available. Stations 313 and 950 began recording results in the fall of 2001 and have only about 44 000 hourly records, and are not included in the goodset data. The other stations have about 57 000 hourly records, which compose the goodset data. We have selected the month of June to reduce the effects of seasonal changes and avoid the summer monsoon and synoptically active winter periods.

We analyze all of the stations within a 40-km radius of the Busan and Daegu synoptic stations, corresponding to 18 stations for both regional networks. Busan is located on the southeast coast of the Korean Peninsula. The orography of the region is dominated by four main features: 1) the sea, 2) a coastal plain, 3) two mountain ranges with maximum elevations of 801 and 659 m, and 4) valleys that sometimes include an extension of the urban areas inland and major rivers. The Daegu regional network is more agricultural with flatter topography. Both networks contain about 10% urban area, which is centered on Busan and Daegu.

Assessment of the spatial variations of the wind field with more complex surface conditions, including urban

areas, is difficult because the horizontal gradients occur on a variety of horizontal scales (Kanda 2006). In urban areas or areas with variable tall vegetation, the wind sensor is often in the roughness sublayer, in which case

1) the wind observation represents only a relatively small microarea, and
2) horizontal gradients are contaminated by the inability to measure at the same relative height at each station.

Although the observational level is preferably above the roughness sublayer (Roth 2000), determination of the depth of the roughness sublayer is not always possible. As a result, the vertical gradients contaminate the computed horizontal gradient across the network.

These problems occur with the present networks even though the stations were generally deployed over open, level terrain on the microscale and at a horizontal distance of at least 10 times the height of any nearby building. This was carried out using 10- and 20-m towers. This strategy reduced the influence of individual obstacles, but led to differences in the sensor height with respect to absolute ground level. Wind speed and direction are measured with two different types of cup anemometers and vanes. Wind speed accuracies range from 0.3 to 0.5 m s^{-1}, and direction accuracies range from 3° to 5°, depending on the particular model type and wind speed.

3. Between-station correlations in the Busan network

The coherency between stations will be examined in terms of the correlation of the u and v components between stations for all the possible two-station combinations. These between-station correlations will be examined as a function of station separation distance. The correlations for the u and v components are combined as

$$R_{uv} \equiv \left[\frac{(R_u^2 + R_v^2)}{2}\right]^{0.5}, \quad (1)$$

where R_u and R_v are the correlation coefficients for individual components. Scaling by 2 ensures that R_{uv} ranges between -1 and 1.

The between-station correlation for all station combinations averages only 0.40 for the u component, 0.42 for the v component, and 0.42 for the combined correlation [Eq. (1)]. These low correlations underscore the strong spatial variability over the Busan area. Such spatial variation can be large even over urban areas with minimal topography (Hanna et al. 2007). The individual between-station correlations in the Busan regional network are all below 0.8.

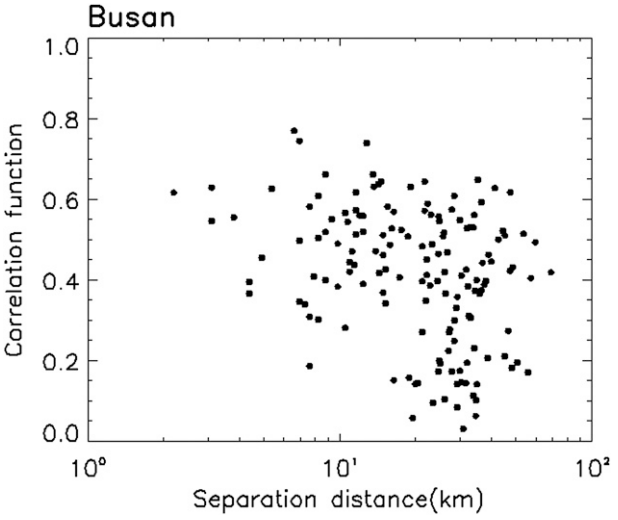

FIG. 2. Between-station correlations for all of the pairs of stations for the goodset data as a function of separation distance between stations based on 8 yr of June data within the Busan regional network.

The correlation between pairs of individual stations as a function of separation distance between stations is shown in Fig. 2. The between-station correlations begin to decrease when the separation distance becomes larger than about 20 km, albeit with large scatter. The scatter is large relative to that over grassland for selected stationary periods (Hanna and Chang 1992). For complex topography with embedded urban subareas, the station separation distance is only one of the significant factors. Stations close to each other (less than 10 km) may be characterized by small between-station correlations (Fig. 2). As an example, stations 159 and 160 in the Busan regional network are less than 5 km apart, but have a combined correlation of only $R_{uv} = 0.56$. The correlation is reduced by the fact that station 160 is 518 m above sea level, the highest in the network, while the surface elevation of station 159 is 69 m. As a second example, stations 938 and 941 have a correlation of only 0.30 even though they are only 8 km apart. These two stations are in separate valleys. Their wind roses are completely different (Fig. 3). The winds at station 938 are primarily from the north or south probably because of the channeling effects of the valley. Winds at station 941 are primarily from the southeast, presumably because of the mountain barrier to the east. The relatively small correlations between stations imply that the wind at a given point cannot be estimated by interpolating winds from the nearest stations.

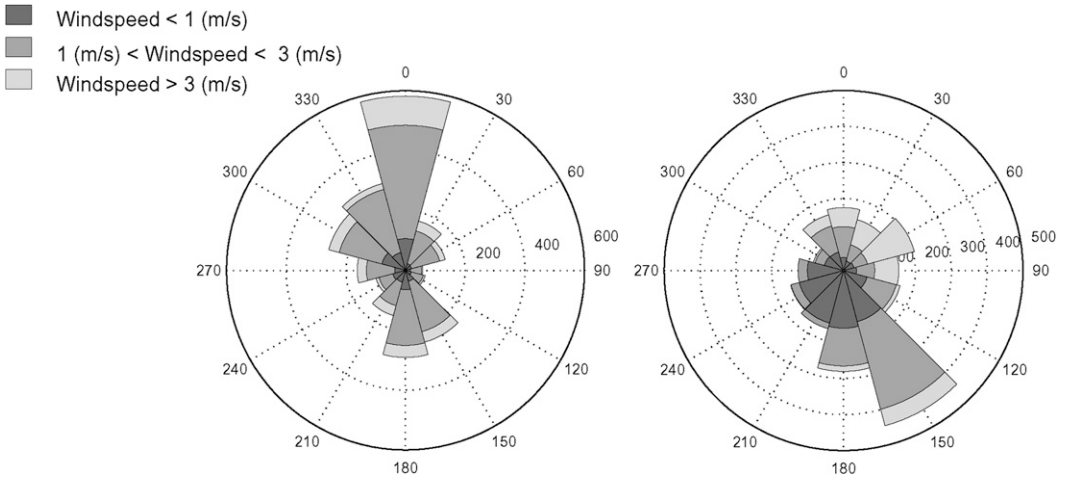

FIG. 3. Wind roses for stations 938 and 941 for June. Winds at both stations are channeled by the topography.

For a given station, the between-station correlation coefficient is now averaged over all of its station pairs in the network. The highest between-station correlation in the Busan network is for the coastal station 937 with a coefficient of 0.56. This station could be considered as the most representative station, or the best one-station index, for the region, although the correlations with the other stations are still relatively low. The regional average between-station correlations for stations 910, 940, and 942 also exceed 0.5. Station 925, which is an inland station among low hills, has the smallest average between-station correlation, only 0.22. This station represents a different wind regime relative to the rest of the Busan regional network even though it physically lies within the network.

For weak winds (network-averaged wind less than 2 m s^{-1}), the correlations are even smaller (Fig. 4), although the dependence of the between-station correlation on the separation distance between stations remains significant. For some station pairs, the winds are completely uncorrelated. With weak winds, thermally generated flows and the micrometeorological setting both become more important and the vertical mixing between the ambient flow and the surface is weak.

4. The mesovelocity scale for the Busan network

To quantify the variability of the wind within the network, we define the mesovelocity scale for each hour (Mahrt et al. 2009, manuscript submitted to *Quart. J. Roy. Meteor. Soc.,* hereinafter MTP) as

$$V_{\text{meso}} \equiv [u_i^{*2} + v_i^{*2}]^{1/2}, \tag{2}$$

where the square brackets define an average over the network, the subscript i refers to the ith station, and

$$u_i^* = u_i - [u_i] \tag{3}$$

is the deviation of u at station i from the network-average wind component. Recall that the winds are 1-h-averaged values. The mesovelocity scale rarely decreases below 0.5 m s^{-1} for the Busan network. Even when the large-scale flow is nearly calm, there are always local circulations, partly driven by differential heating–cooling patterns associated with the topography, variations of land use, and land–sea contrasts. In contrast, the speed of the network vector-averaged wind,

$$V_{\text{network}} = ([u_i]^2 + [v_i]^2)^{1/2}, \tag{4}$$

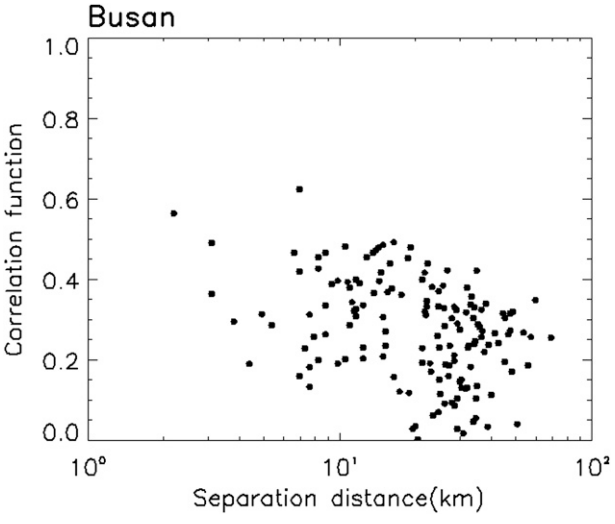

FIG. 4. Between-station correlations for all of the pairs of stations for the goodset data for weak winds (network-averaged wind less than 2 m s^{-1}) as a function of separation distance between stations within the Busan regional network.

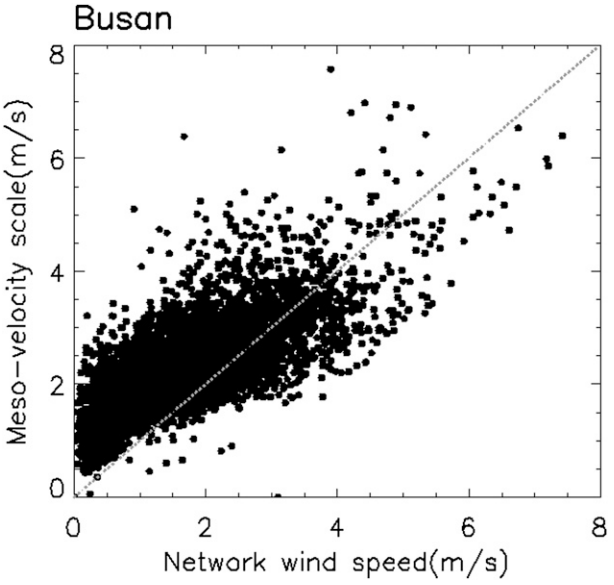

FIG. 5. The mesovelocity scale as a function of the speed of the network vector-averaged wind within the Busan regional network.

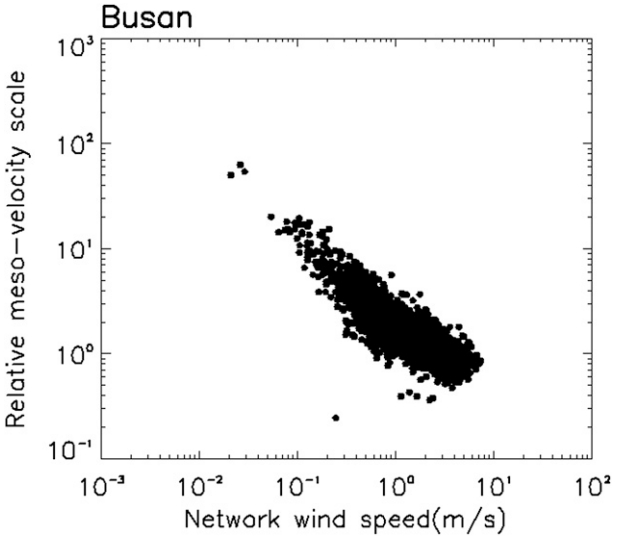

FIG. 6. The mesovelocity scale, scaled by the speed of the network vector-averaged wind, as a function of the speed of the network vector-averaged wind within the Busan regional network.

occasionally reaches very small values on the order of 0.1 m s^{-1} (values less than 0.2 m s^{-1} about 1% of the time). When V_{meso} is significantly larger than V_{network}, the airflow is mainly due to local circulations. The mesovelocity scale is larger than the speed of the network vector-averaged flow for 80% of the records, indicating that the spatial variability of the wind field is typically quite important. For the network-averaged flow greater than 5 m s^{-1}, the mesovelocity scale is greater than the speed of the network-averaged flow only about 15% of the time.

The mesovelocity scale increases with the speed of the network vector-averaged wind, at a rate that is less than linear and with large scatter (Fig. 5). The large scatter suggests that the strength of the large-scale flow is only one of the significant processes affecting the spatial variability. The relative mesovelocity scale,

$$\text{RV}_{\text{meso}} = \frac{V_{\text{meso}}}{V_{\text{network}}}, \tag{5}$$

decreases with increasing wind speed and shows less scatter, partly due to self-correlation (Fig. 6).

The above mesovelocity scale, defined in terms of the spatial variation of the wind field, behaves differently than the mesovelocity scale defined in terms of within-hour time variations at a fixed station, as examined in Anfossi et al. (2005) and Mahrt (2007). The mesovelocity scale based on time variation tends to be on the order of 1 m s^{-1} and does not generally increase with increasing wind speed. Such time variation is due to transient mesoscale motions, which are not significantly enhanced by increasing wind speed. In contrast, the topography includes spatially varying perturbations that increase with increasing wind speed and therefore increases the mesovelocity scale based on spatial variations.

5. Comparison between inland and coastal zone networks

The behavior of the mesovelocity scale is now contrasted between the strongly heterogeneous coastal

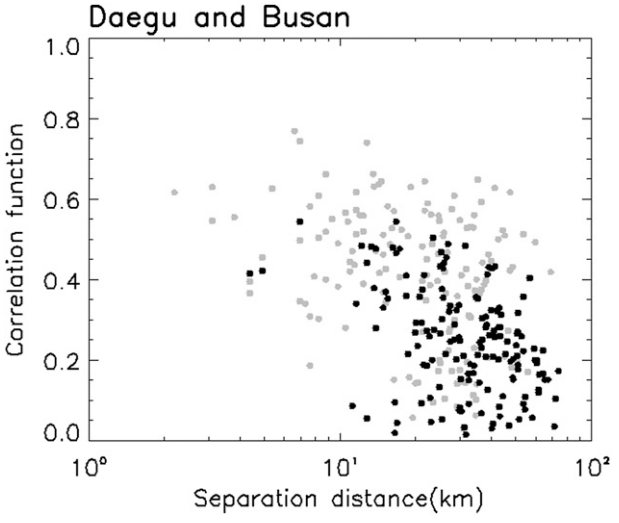

FIG. 7. As in Fig. 2 but for the Daegu regional network (black dots); the gray dots are the Busan network.

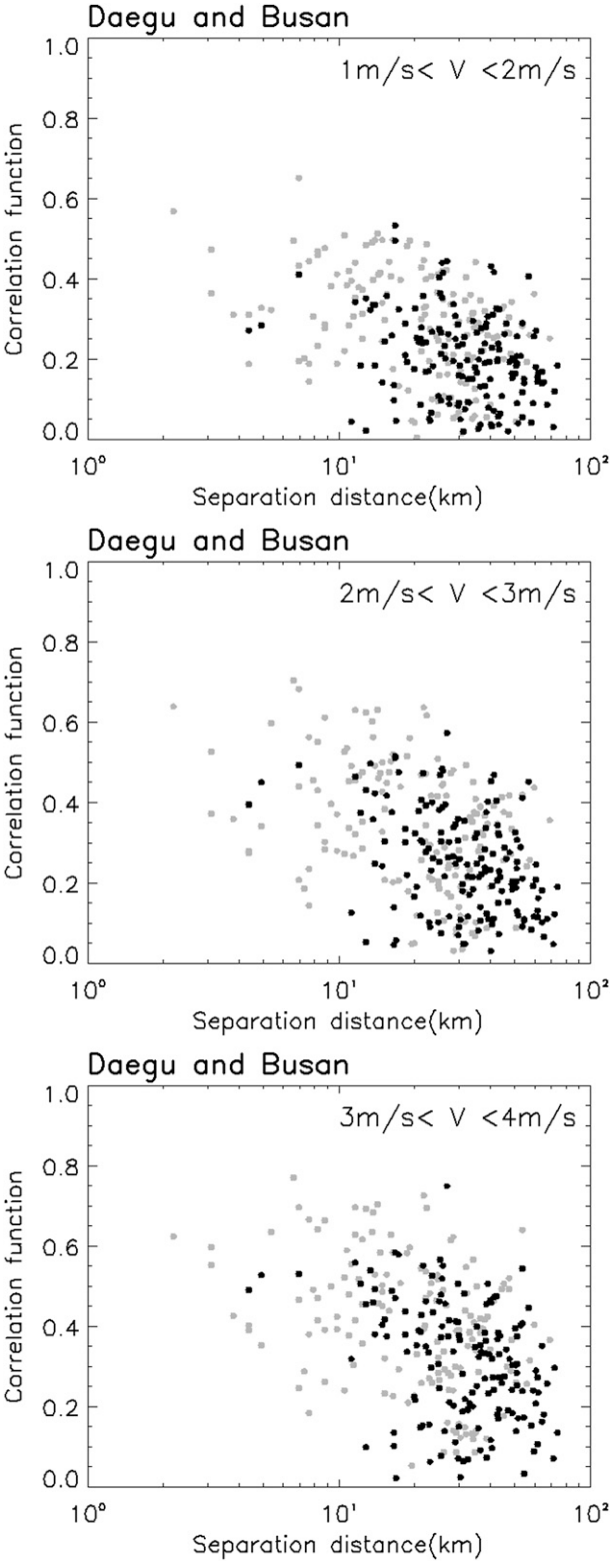

FIG. 8. As in Fig. 7 but for specified wind speed intervals.

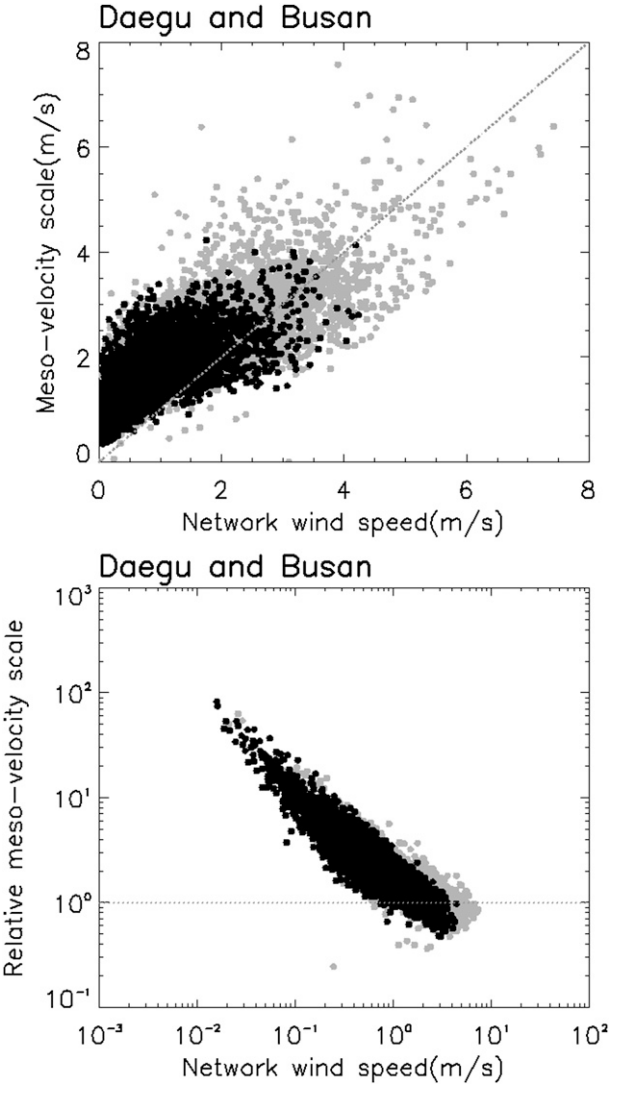

FIG. 9. The mesovelocity scale and relative mesovelocity scale as a function of the speed of the network vector-averaged wind for the Daegu (black dots) and Busan regional networks (gray dots).

zone (Busan regional network) and the moderately heterogeneous inland network (Daegu region). Figure 7 shows that the scatter in the correlation coefficient as a function of separation distance is less over the less heterogeneous Daegu regional network. However, the individual between-station correlations in the Daegu regional network are smaller than those in the Busan network, which are all below 0.6. The regional-averaged between-station correlations are a little less than 0.35. The smaller correlations in the Daegu network may be due to weaker large-scale flow, compared to the Busan network, and the network-scale organization by the land–sea contrast in the Busan network. For the same wind speed interval, the between-station correlation

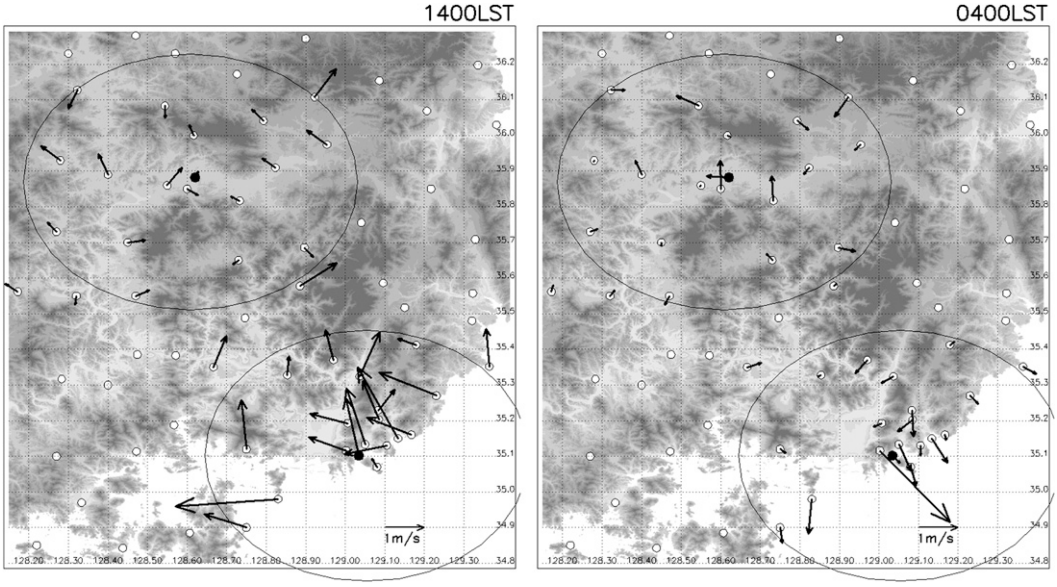

FIG. 10. The horizontal distributions of wind vectors at 1400 and 0400 LST for the Daegu (upper circle) and Busan (lower circle) regional networks.

in both networks is compared (Fig. 8). This result shows higher correlations under higher wind speeds and for a given wind speed interval and that the correlations tend to be slightly higher for the Busan network.

The mesovelocity scale increases with wind speed for both networks, but with considerable scatter (Fig. 9, top). The mesovelocity scale increases wind speed more slowly than a linear scalesuch that the relative mesovelocity scale decreases with wind speed (Fig. 9, bottom). The dependence of the mesoscale velocity on wind speed is similar for both networks. Overall, the mesovelocity scale is greater for the Busan regional network partly because the winds are generally stronger.

The resultant wind vectors averaged over the dataset for 1400 LST (Fig. 10) reveal strong marine air penetration at the coast with weaker upvalley–upslope flow farther inland. Conversely, the resultant winds for 0400 LST show weak to moderate offshore flow and downslope–downvalley flow farther inland. The highest coastal station shows much stronger offshore flow, suggestive of a deep layer of nocturnal offshore flow originating from a large inland area. As compared with the Busan network where the land–sea contrasts organize the flow, the nocturnal winds for the Daegu network are more likely determined by local features and the coherence across the network is less. Even though the heterogeneity for the Daegu network is not dramatic, it can dominate the flow variation.

On average, the spatial variations of the wind field are as large or larger than the network-averaged winds for both the Busan and Daegu networks. Over more homogeneous regions, the mesovelocity scale is expected to be substantially smaller. As an example, we show the dependence of the mesovelocity scale on wind speed for the relatively flat Iowa network (Fig. 11), the crops consisting primarily of soybeans and maize (MTP). Here, the mesovelocity scale is closely related to the wind speed with a typical value of about 0.25 of the wind

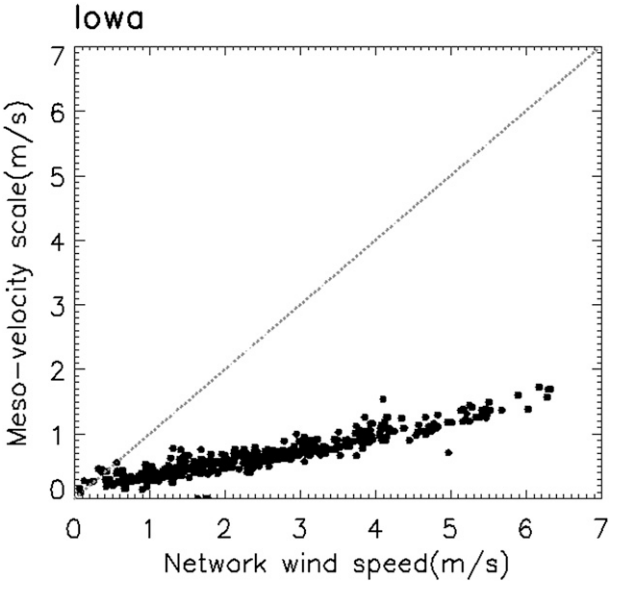

FIG. 11. The mesovelocity scale as a function of network averaged wind speed for the Iowa network.

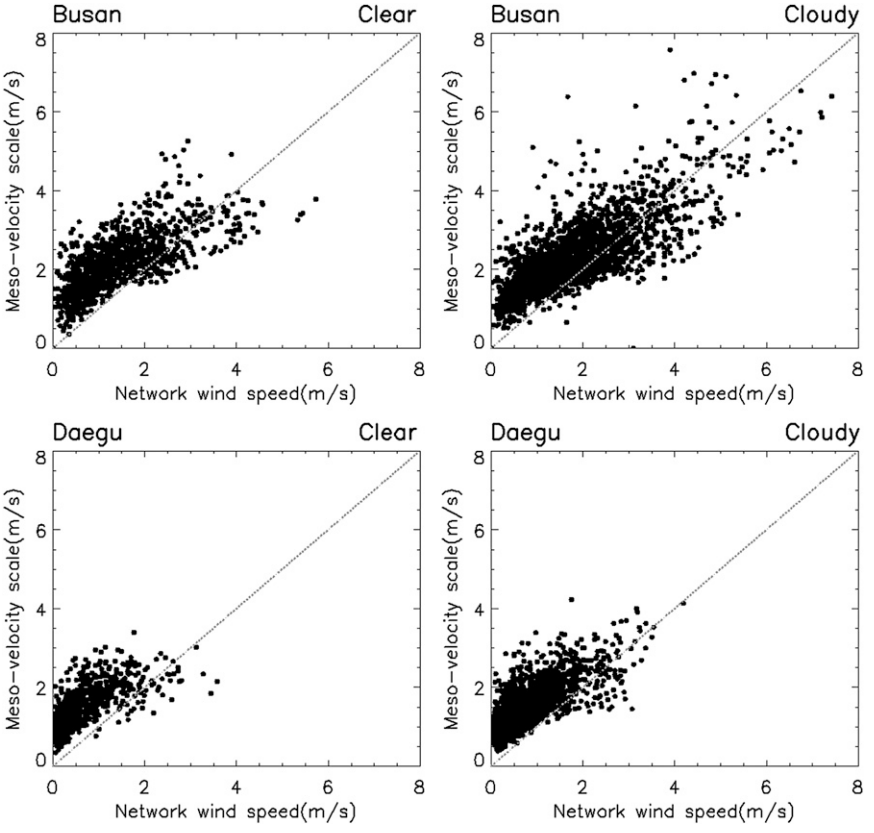

FIG. 12. The mesovelocity scale as a function of wind speed for clear and cloudy periods: the (top) Busan and (bottom) Daegu networks.

speed. For other relatively homogeneous networks that we have examined (e.g., Kustas et al. 2004; MTP), the mesovelocity scale is typically about 25% of the wind speed, although the scatter may be much greater than in Fig. 11.

We now investigate the influences of cloudiness on the wind field. Clear skies with daytime surface heating and nocturnal cooling increase the potential for buoyancy-driven slope flows. Each of the centers of the Busan and Daegu networks contains a synoptic station with cloud cover measurements. We divide the data into mostly clear conditions with cloud cover of 20% or less and mostly cloudy conditions with cloud cover of 80% or more. The mesovelocity scale tends to be larger for mostly clear conditions relative to cloudy conditions for both networks (Fig. 12), suggesting that thermally driven circulations increase the mesovelocity scale and increase the scatter in the relationship between the mesovelocity scale and the wind speed. These tendencies occur for both daytime and nocturnal conditions (Fig. 13).

The resultant wind vectors (Fig. 14) also show the stronger influence of local slopes and the land–sea contrast for clear-sky conditions, relative to cloudy conditions. The winds for cloudy conditions at 1400 LST are southeasterly over much of the Busan network. However, with clear skies, the southeasterly flow is much stronger near the coast, apparently due to enhancement by marine air penetration. In addition, the wind direction for clear-sky conditions is more strongly influenced by local topography relative to cloudy conditions. As an aside, the marine air has not yet penetrated into the inland valleys at 1400 LST.

For nocturnal conditions (Fig. 14), the inland wind field in the Busan network is more closely tied to the local topography than near the coast and does not systematically participate in the offshore flow, although some valleys may feed the offshore flow.

6. Conclusions

In this study, we examined the spatial variations of the wind fields observed in the Busan and Daegu regional networks. Two-point correlations of the wind fields sometimes revealed only weak coherency between stations, suggesting that smaller station spacing is required. This problem is predictably most significant with weak

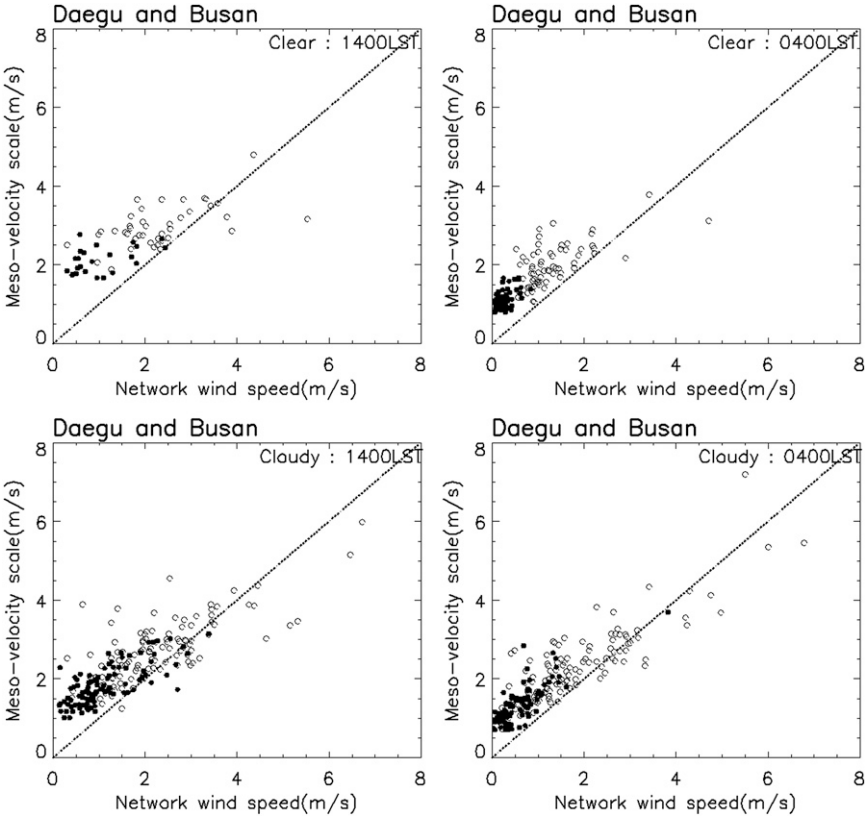

FIG. 13. The mesovelocity scale as a function of wind speed for clear and cloudy periods for 1400 and 0400 LST. Black dots and open circles indicate the Daegu and Busan regional networks, respectively.

winds, clear skies, and significant topography. The relatively small correlations between stations imply that the wind at a given point cannot be estimated by interpolating winds from the nearest stations.

A mesovelocity scale was defined in terms of the spatial variability of the wind within the network. For the Busan regional network, the mesovelocity scale is typically the same order of magnitude as the speed of the network-averaged wind, revealing the large spatial variability of the wind field within this network. In contrast, the mesovelocity scale averages about 25% of the wind speed over the relatively homogenous Iowa network.

The spatial variability of the wind field increases systematically with the speed of the network-averaged wind, especially for the Busan network, which has stronger topography. Evidently, the topography induces stronger wind perturbations with stronger winds.

Significant scatter in the relationship between the spatial variability of the wind field and the wind speed appears to be partly related to thermally generated flows. The magnitude of the mesovelocity scale is generally larger for clear conditions compared to cloudy conditions for both the Busan and Daegu regional networks. This result suggests that thermally driven circulations increase the mesovelocity scale and increase the scatter in the relationship between the mesovelocity scale and the wind speed. Resultant wind vectors indicate much different flow patterns between clear and cloudy conditions. Case studies are required to more clearly separate the influences of ambient flow conditions, cloud cover, slope circulations, and land–sea contrasts.

The above results identify the complexity of the flow statistics and demonstrate that current network strategies are inadequate for the examination of the multiple physical influences. Since it is difficult to separate out the spatial variations on the network scale and the influences of micrositing of a given station, we recommend deploying a small micronetwork about one or more of the stations.

Acknowledgments. This work was supported by a grant of ''Eco-Technopia 21 Project'' from the Ministry of Environment of Korea and the Brain Korea 21 Project.

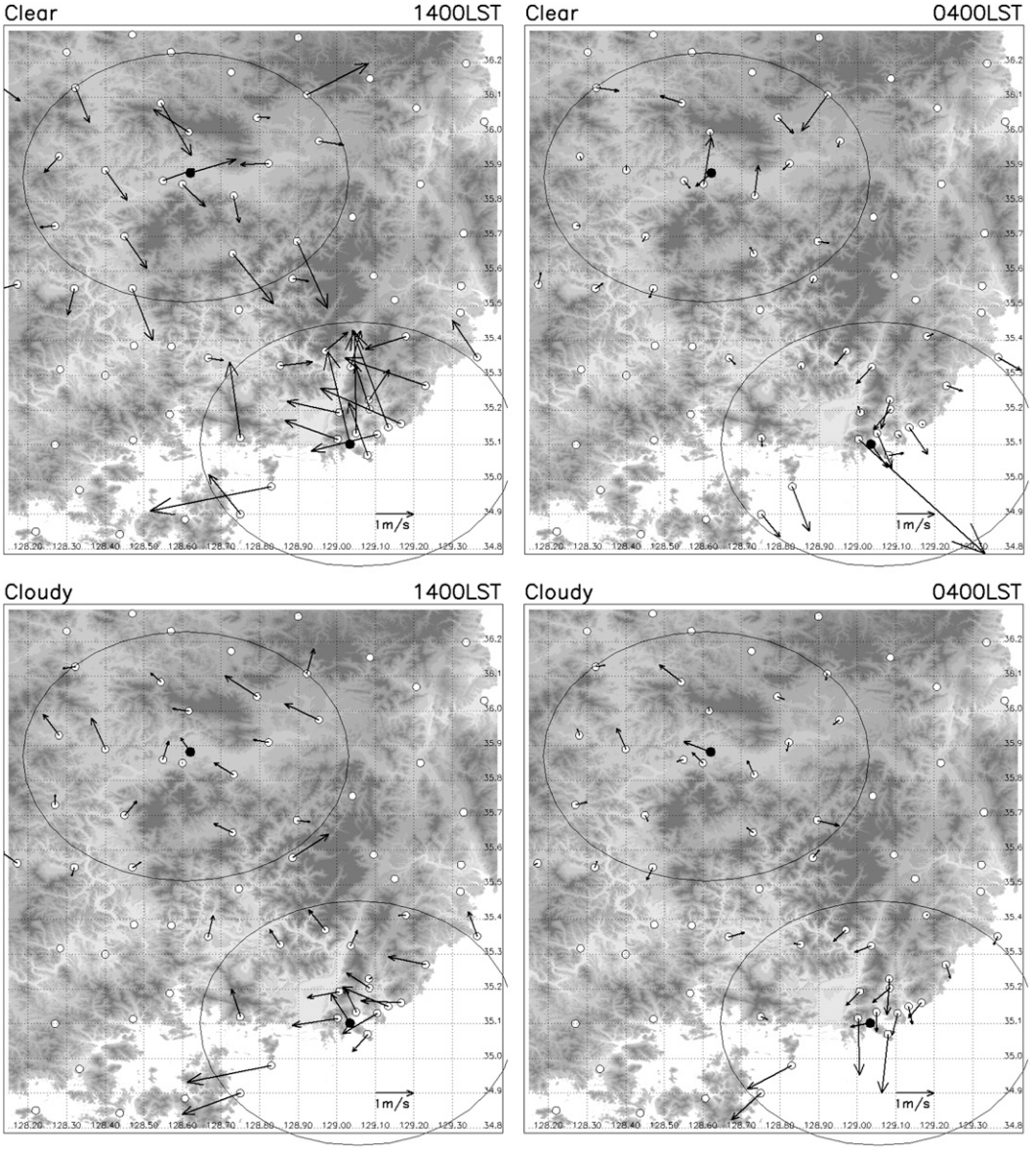

FIG. 14. As in Fig. 10 but for clear days at 1400 and 0400 LST for the Daegu (upper circle) and Busan (lower circle) regional networks.

We are grateful to the Korea Meteorological Administration for providing the AWS meteorological data.

REFERENCES

Anfossi, D., D. Oettl, G. Degrazia, and A. Boulart, 2005: An analysis of sonic anemometer observations in low wind speed conditions. *Bound.-Layer Meteor.,* **114,** 179–203.

Beaver, S., and A. Palazoglu, 2006: Cluster analysis of hourly wind measurement to reveal synoptic regimes affecting air quality. *J. Appl. Meteor. Climatol.,* **45,** 1710–1726.

Garratt, J. R., 1990: The internal boundary layer—A review. *Bound.-Layer Meteor.,* **50,** 171–203.

Grimmond, C. S. B., and T. R. Oke, 2002: Turbulent heat fluxes in urban areas: Observations and Local-Scale Urban Meteorological Parameterization Scheme (LUMPS). *J. Appl. Meteor.,* **41,** 792–810.

Ha, K.-J., E.-H. Jeon, and H.-M. Oh, 2007: Spatial and temporal characteristics of precipitation using an extensive network of ground gauge in the Korean Peninsula. *Atmos. Res.,* **86,** 330–339.

Hanna, S., and J. Chang, 1992: Representativeness of wind measurements on a mesoscale grid with station separations of 312 m to 10 km. *Bound.-Layer Meteor.,* **60,** 309–324.

——, J. White, and Y. Zhou, 2007: Observed winds, turbulence, and dispersion in built-up downtown areas of Oklahoma City and Manhattan. *Bound.-Layer Meteor.,* **125,** 441–468.

Kanda, M., 2006: Progress in the scale modeling of urban climate. *Theor. Appl. Climatol.,* **84,** 23–33.

Kastner-Klein, P., and M. Rotach, 2004: Mean flow and turbulence characteristics in an urban roughness sublayer. *Bound.-Layer Meteor.,* **111,** 55–84.

Kustas, W. P., F. Li, T. J. Jackson, J. H. Prueger, J. I. MacPherson, and M. Wolde, 2004: Effects of remote sensing pixel resolution on modeled energy flux variability of croplands in Iowa. *Remote Sens. Environ.,* **92,** 535–547.

Ludwig, F. L., J. Horel, and C. D. Whiteman, 2004: Using EOF analysis to identify important surface wind patterns in mountain valleys. *J. Appl. Meteor.,* **43,** 969–983.

Mahrt, L., 2000: Surface heterogeneity and vertical structure of the boundary layer. *Bound.-Layer Meteor.,* **96,** 33–62.

——, 2007: Weak-wind mesoscale meandering in the nocturnal boundary layer. *Environ. Fluid Mech.,* **7,** 331–347.

——, C. K. Thomas, and J. H. Preuger, 2009: Space–time structure of mesoscale modes in the stable boundary layer. *Quart. J. Roy. Meteor. Soc.,* **135,** 67–75.

Pino, D., J. Vila-Guerau de Arellano, A. Comeron, and F. Rocadendosch, 2004: The boundary layer growth in an urban area. *Sci. Total Environ.,* **334–335,** 207–213.

Roth, M., 2000: Review of atmospheric turbulence over cities. *Quart. J. Roy. Meteor. Soc.,* **126,** 941–990.

Staebler, R. M., and D. R. Fitzjarrald, 2004: Observing subcanopy CO_2 advection. *Agric. For. Meteor.,* **122,** 139–156.

Steyn, D. G., 2002: Scaling the vertical structure of sea breezes revisited. *Bound.-Layer Meteor.,* **107,** 177–188.

Whiteman, C. D., 2000: *Mountain Meteorology*. Oxford University Press, 355 pp.